

RECENT RESULTS ON DIRECT PHOTON PRODUCTION AT CERN

presented by

E. LANCON

DPhPE-SEPh, CEN - SACLAY



ABSTRACT: Recent results in the study of high P_T direct photons from the experiments NA24, R808, UA2 and WA70 are reviewed. Studies of correlation of particles associated with high P_T direct photons and beam dependence of direct photons production are presented. Ratios of γ to π^+ and γ to jet productions as well as cross-sections are also presented.

I. INTRODUCTION

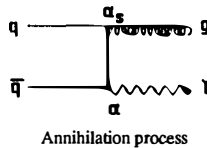
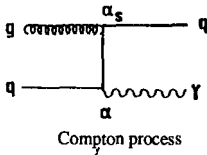
Since the discovery of prompt photon (often called direct photon) production at the ISR there has been a growing interest in studying this process.

The study of scattering processes with large transverse momentum (P_T) is a convenient way to extract information on hadron constituents (quarks and gluons) and their interactions¹). The advantages of selecting high P_T direct photon final states in the hard scattering of hadron constituents can be briefly recalled:

- the number of parton processes involved is small (2 at first order)
- the coupling of a photon to a quark is well understood
- the photon directly participates in the collision and can be detected whereas quarks and gluons fragment into hadrons
- no fragmentation effects are present making the results directly comparable to the theory with no need of a fragmentation model.
- the kinematics (angle and energy) of the outgoing parton, photon in our case, is measured with a good precision.

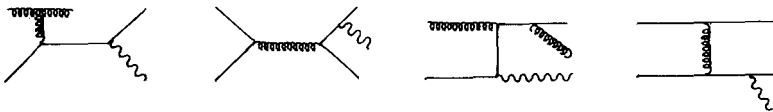
At first order in α_s , direct photons are produced through two processes : the inverse QCD

Compton process: $qg \rightarrow \gamma g$ and the annihilation: $q\bar{q} \rightarrow \gamma g$. One feature of direct photon production is that a gluon is present in both processes, either in the initial state (Compton) or in the final state (Annihilation).



If the contributions from these two first order graphs can be separated, prompt photon production may allow a study of the gluon distribution within hadrons and jet fragmentation.

Prompt high P_T photons may also be produced by many bremsstrahlung diagrams like the following :



These contributions as well as the next-to-leading order in α_s contributions have been calculated^{2,3}). All together these contributions increase the prompt photon cross-section by a factor of the order of 1.5 to 2, depending on the kinematic configuration.

Experimentally the detection of direct photons is not easy for several reasons. The yield of single photon relative to jets is smaller by several orders of magnitude ($\approx 10^{-4}$) because the photon production is reduced by a factor \propto/α_s compared to jets and many more graphs and colour factors contribute to the jet yield. There is a large background resulting from π^0 and η decays into photons, which implies a difficult measurement of the direct photon signal. This background follows from two effects. The first effect is that one of the photons from a $\pi^0, \eta \rightarrow \gamma \gamma$ decay may not be detected, either because it is outside the detector acceptance or because it has a too low an energy; the other photon then appears as a direct photon. This is the main source of background at low momentum. At high momentum, the two photons from a π^0, η decay (or at very high P_T several neutral particles belonging to the same jet), have too small a spatial separation to be resolved in the detector and appear as a single photon. Beside this background in nearly all direct photon experiments, beam halo or μ bremsstrahlung (in fixed target experiments) fakes direct photons.

However because prompt γ contrarily to π^0 and eta do not issue from a parton fragmentation, we expect, that at fixed \sqrt{s} the ratio γ/π^0 should increase with P_T . Then working at high P_T makes the measurement easier (although in this region the statistics are poor). Several other effects contribute to the increase of the γ/π^0 ratio with P_T : the fragmentation function becomes softer as the parton process becomes harder, the gluon distribution within hadrons becomes smoother, reducing the contribution of graphs like $gg \rightarrow gg$ to the jet (π^0) yield and the strong coupling constant α_s decreases with the hardness of the collision.

Two different techniques have been employed to extract the direct photon signal and suppress the huge background resulting from non-prompt photon sources (e.g. π^0, η ... decays, non-resolved neutral multi-particle states) and hadrons misidentified as γ 's (e.g. K_L^0 , neutrons ...).

In the first one, called the "Direct Method" a prompt photon is defined as a photon not coming from an identified decay (e.g. $\pi^0 \rightarrow \gamma \gamma, \dots$). A large fraction of π^0 and η are recognised by reconstructing the two photon mass. From a knowledge of the detector acceptance and the observed rate of π^0 and η , most of the background can be evaluated. The direct photon signal is then calculated from the excess of observed photons over the calculated background. Detectors should be designed to have good efficiency in resolving π^0 's or η 's and good acceptance in order to minimize the number of lost decay photons. This method is limited at high P_T , where the two photons separation is comparable to the detector granularity, most of the decays cannot be resolved.

In the second technique called the "Conversion Method", π^0 's and η 's are not reconstructed and a direct photon candidate is defined as a neutral energy deposition in the calorimeters. The fraction

of direct photons is determined statistically by measuring the conversion rate in a preshower detector. A signal, in this detector more likely occurs for two coalescing photons than for a single one. This technique requires a precise knowledge of the conversion probability in the preshower detector and of the energy loss in the converter. The later requirement is needed when comparing the steeply falling spectra of converted and non-converted photons.

In the following, I shall review recent prompt photon production results exclusively from four experiments. NA24⁴⁾ and WA70⁵⁾ are two SPS fixed target experiments using 300 GeV/c and 280 GeV/c beams (π^- , π^+ , P) respectively interacting on a hydrogen target. R808⁶⁾ is an experiment studying PP and $P\bar{P}$ collisions at a center of mass energy $\sqrt{s} = 53$ GeV at the ISR using the A.F.S. detector⁷⁾. UA2⁸⁾ operates at the SPPS collider studying $P\bar{P}$ collisions at $\sqrt{s} = 630$ GeV.

These four experiments measure prompt γ production in the complementary kinematic regions given in Table 1.

Before presenting the results, I shall briefly describe the experimental features relevant for the analysis presented here.

II. EXPERIMENTAL SET-UP

Three among the four experiments mentioned above have observed direct photon production by employing the direct method (NA24, R808, WA70), while UA2 uses the conversion method.

The three experiments using the direct method require a fine granularity photon detector in order to separate the two γ 's from π^0 or η decays (especially for fixed target experiments).

The NA24 photon detector⁹⁾ is 9.6 radiation lengths (X_0) thick and consists of alternate layers of lead sheets and proportional tubes ($0^\circ, 90^\circ$ and 45° inclination). The photon detector is followed by the NA5 calorimeter which consists of an electromagnetic ($16X_0$) and a hadronic (6λ) part. An iron wall and a veto counter array located upstream of the detector safeguard the experiment against upstream interactions and muon background.

The WA70 photon detector¹⁰⁾ consists of an electromagnetic calorimeter made of lead sheets interleaved with teflon tubes filled with liquid-scintillator. This detector is $24X_0$ deep and segmented longitudinally in 3 parts ($8X_0$ each). Tubes are arranged orthogonally and an electronic time of flight system is used to resolve spatial ambiguities and reject backgrounds.

The R808 photon detector¹¹⁾ is provided by two opposite walls of NAI blocks, $5.3 X_0$ deep. This detector is located inside an uranium calorimeter consisting of a $6 X_0$ electromagnetic part and a 3.6 absorption length hadronic part.

Table 1 shows, the energy resolution and the π^0 mass resolution achieved by these experiments.

In the UA2¹²⁾ experiment the conversion method is used to measure the direct photon signal. Two measurements have been performed: in the central region at a mean pseudorapidity $\eta=0$ and in the Forward/Backward regions : $1.1 \leq |\eta| \leq 1.7$. These measurements rely on preshower detectors which consist of a $1.5 X_0$ converter followed by a multi-wire proportional chamber in the central part and a $1.4 X_0$ converter followed by a multi-tube proportional chamber in the Forward/Backward regions. The chamber thresholds are set to 2 minimum ionizing particles deposit (mips) and 6 mips for the central and the Forward/Backward detectors respectively. In both cases, the photon energy is measured using calorimeters located behind the preshower detectors.

III. DATA SELECTION AND ANALYSIS

For NA24, R808 and WA70 experiments details of the analysis can be found in previous publications¹³⁾, and they are only briefly recalled here. These experiments using the direct method have similar criteria to select prompt photons. In each event, electromagnetic showers, are paired; if the invariant mass of the pair is found to be consistent within errors with the π^0 (η) mass, the pair is assumed to originate from a π^0 (η) decay. An electromagnetic shower which could not be paired is considered to be a direct photon candidate. The background to direct photon candidates is estimated from Monte-Carlo generated π^0 and η events. Depending on P_T it is due to : i) photons from π^0 and η decays for which one of the photons escapes detection (limited detector acceptance) or is not reconstructed due to its low energy and ii) coalesced showers from unresolved π^0 decays. The observed γ and π^0 samples must finally be corrected by their relative detection efficiency to give the final observed γ/π^0 ratio.

NA24 EXPERIMENT

Events are selected off-line by requiring that the direction of the triggering shower (as determined by the shower development measurement in the photon detector) points to the target, the total energy measured be consistent with the beam energy and that the calorimeter timing (using Flash ADC's) agrees with the time at which the interaction took place. These cuts remove most of the pile up and muon background.

WA70 EXPERIMENT

Cuts are used to remove pile up and muon background. The shower direction as given by the calorimeters must point to the target and the time-of-flight information must agree with the time of the incident particle.

The ratio γ/π^0 and estimated background are shown in Fig.1.a for WA70 and Fig.1.b for NA24.

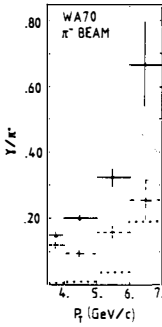


Fig. 1.a: Ratio γ/π^* for incident π^* . Background contribution due to halo (...) and total (---) background are shown.

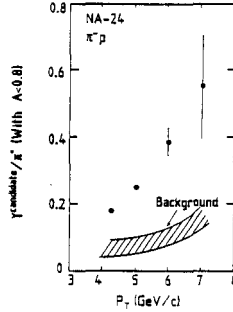


Fig. 1.b: The ratio of γ candidate/ π^* and the Monte-Carlo estimated background (dashed area).

R808 EXPERIMENT

Background originating from cosmic rays and beam-gas interactions is rejected by requiring a vertex from charged particles in the crossing region and correct timing in hodoscopes located near the beam. The background for the detection of direct photons has been evaluated from Monte-Carlo calculation. The different contributions are shown in Figure 2 as a function of P_T .

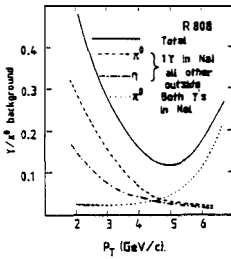


Fig. 2.a: Contributions to γ/π^* background.

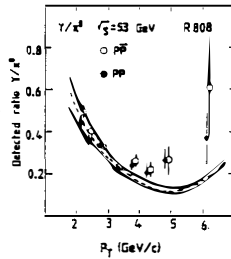


Fig. 2.b: Observed γ/π^* ratio. The dashed line is the sum of all background contributions.

UA2 EXPERIMENT

In the P_T range considered (10-50 GeV/c), π^0 decays cannot be resolved and a large background from jets containing unresolved neutral multi-particles is present. However such backgrounds are generally accompanied by other jet fragments whereas direct photons are expected to be well-isolated.

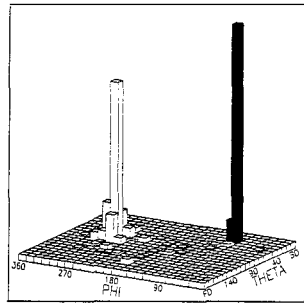


Fig. 3: $\theta-\theta$ energy flow plot of a direct photon candidate in UA2. The energy of the direct photon candidate is shown in black, the away side jet is clearly seen (white towers).

Therefore a direct photon candidate is defined as an electromagnetic energy deposition in the calorimeters without any associated charged track and satisfying isolation criteria. Energies are corrected for losses in the preshower detector.

Figure 3 shows the "lego" plot of a typical direct photon candidate in UA2. Beam halo background is removed by requiring: i) that small angle hodoscopes and calorimeter signals occur at the correct time, ii) that the missing transverse momentum of each event be less than 80% of the photon candidate transverse momentum.

The isolation criteria are:

In the central region :

- no charged track and at most one preshower signal may be found in a cone of $\sqrt{\Delta\eta^2 + \Delta\phi^2} < 0.35$ about the cluster direction
- the pattern of calorimeter photomultiplier signals must be consistent with the pattern expected for a single photon

In the Forward/Backward regions :

- no charged track may point to the cluster
- the total energy of all charged and neutral particles impinging on the cells adjacent to the cluster must not exceed 0.3 GeV.

The isolation criteria are intended to reject a large fraction of background and select direct photons. Evidence for this effect can be seen in Fig. 4, where the conversion rate observed in the preshower detectors, for isolated events (dots) and non-isolated events (triangles) is plotted, as a function of energy. $\epsilon_{2\gamma}$ and ϵ_{γ} are the conversion probabilities for two unresolved photons and a single photon, respectively. These probabilities are calculated from a Monte-Carlo simulation of the preshower detectors using the EGS¹⁴⁾ program.

As a result of the different thresholds used to define a preshower signal in the central and Forward/Backward regions, ϵ_{γ} behaves differently in the two regions. The simulations correctly describe the response of the preshower detectors to electrons from test beams. In the Forward/Backward regions, they also agree well with the extrapolation of data containing low-energy reconstructed π^0 's¹⁵⁾. Since the observed conversion rate α is between that expected for single and di-photons in both regions, it is clear that both samples have a substantial content of single photon events. The non isolated sample consists mostly of unresolved photon showers resulting from decays. Due to the effect of neutral multi-particle states, the observed conversion rate is slightly higher than $\epsilon_{2\gamma}$. The calculation of $\epsilon_{2\gamma}$ assumes that the ratio η/π^0 is 0.6¹⁶⁾.

The direct photon sample contains a residual contamination of unresolved π^0 and η decays or multi neutral particles. Assuming that the contamination is due to single π^0 and η only, the

fractional contamination of the sample, $b(P_T)$ is related to the converted fraction α in the sample by:

$$b(P_T) = (\alpha - \epsilon_\gamma) / (\epsilon_{2\gamma} - \epsilon_\gamma)$$

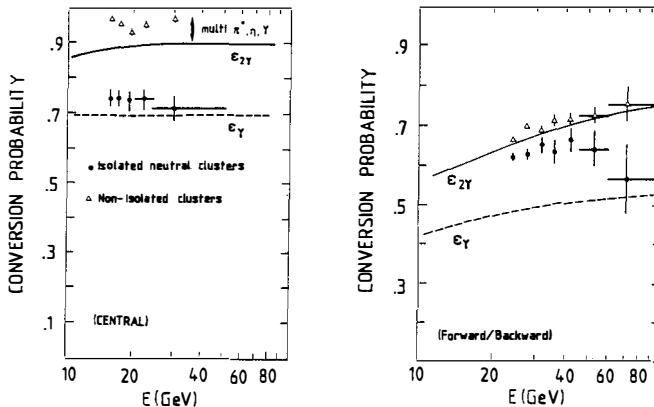


Fig. 4: The conversion probability in the UA2 preshower detectors as a function of energy. The dots represent the conversion probability for the selected photon candidates and the triangles represent the conversion probability for candidates that fail the isolation criteria.

A pure sample of direct photons ($b=0$) would give an observed conversion rate $\alpha = \epsilon_\gamma$, whereas a pure sample of π^0 's and η 's ($b=1$) would give $\alpha = \epsilon_{2\gamma}$. The contribution of unresolved multi- π^0/η states has the effect of increasing $\epsilon_{2\gamma}$. This contribution is evaluated using the ISAJET¹⁷) program. The resulting background fraction $b(P_T)$ averages to $0.28 \pm 0.09(\text{stat}) \pm 0.04(\text{syst})$ in the central region and to $0.70 \pm 0.06(\text{stat}) \pm 0.04(\text{syst})$ in the Forward/Backward regions. The systematic errors come mainly from the evaluation of the multi- π^0/η states contribution.

Since hadronic collisions produce a number of spectator particles, the isolation criteria induce a loss of real events. The efficiency of the isolation criteria is evaluated from samples of minimum bias events and $W \rightarrow e\nu$ events. The hadron contamination to the direct photon sample has been estimated statistically using the energy deposition in the hadronic calorimeters, to be less than 4% of the γ, π^0 contamination.

IV. RESULTS

IV.1 γ/π^0 RATIO

Although it is not predicted by perturbative QCD, the ratio of direct γ production to π^0 production is one of the favourite quantities quoted by experimenters. This ratio explicitly exhibits

the direct γ signal compared to the estimated magnitude of the background. As mentioned in the introduction, the γ/π^0 ratio should increase with P_T . The reported four experiments, for different reactions and over a large range of center of mass energy, observe such an increase.

Results from NA24, after background subtraction, are shown as a function of P_T in Figure 5.a for πP interactions. Error bars correspond to the statistical error only. Corresponding results from WA70 are shown in Figure 4.b. One can already notice that, at a given P_T , this ratio is slightly higher for πP interactions than for $\pi^+ P$ interactions.

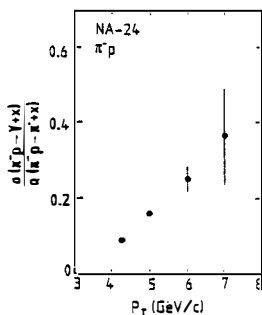


Fig. 5.a: Ratio γ/π^0 for π^- incident beam as measured in the NA24 experiment.

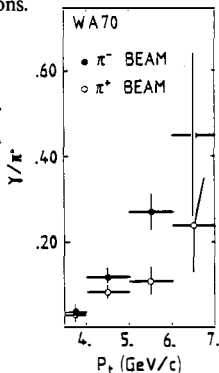


Fig. 5.b: Ratio γ/π^0 for π^+ and π^- beams as measured in the WA70 experiment.

R808 has measured this ratio both for PP and $P\bar{P}$ collisions, it is compared to QCD predictions on Fig. 6. No significant difference is observed between PP and $P\bar{P}$ collisions.

The measurement of the π^0 cross-section made by UA2 in the Forward/Backward regions at $\sqrt{s}=540$ GeV¹⁶ has been repeated at $\sqrt{s}=630$ GeV. The γ/π^0 ratio measured at a mean pseudorapidity of $\langle|\eta|\rangle=1.4$ is displayed, in Fig. 7, as a function of x_T .

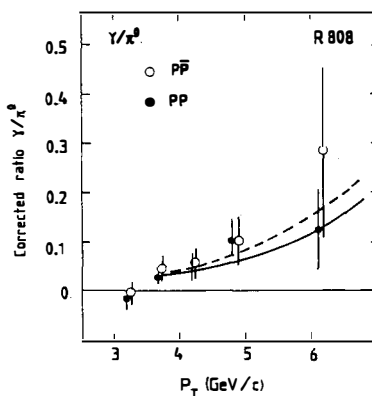


Fig. 6: γ/π^0 ratio in R808. The dashed and solid lines are QCD predictions for this ratio in $P\bar{P}$ and PP interactions given in ref. 18 ($\sqrt{s}=63$ GeV).

This ratio is compared to the ratio measured in $P\bar{P}$ collisions by R808. The increase, at the same x_T , from ISR to collider energy is well predicted by a first order QCD calculation using the

parametrization of structure functions of Ref. 19 and the fragmentation function of Ref. 20. The calculation of the cross-sections ratio at $\sqrt{S}=53$ GeV is shown as the dotted curve.

The same calculation at $\sqrt{S}=630$ GeV is shown as the dashed curve, the effect of scaling violation in the fragmentation function is investigated by repeating the calculation with no such scaling violations (shown as the dotted-dashed curve).

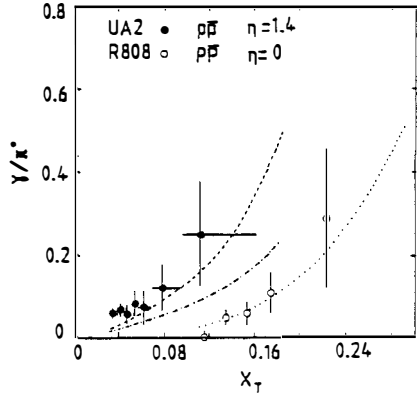


Fig. 7: The ratio γ/π^0 as a function of x_T . The solid points are the result of UA2. The result of R808 is shown as open circles. A set of QCD calculations is also shown (see text).

IV.2. BEAM RATIOS

Using beams of particles and anti-particles, one expects to separate the two main contributions to direct photon production. Because of the large content of valence anti-quarks of π^- , in π^-P collisions the annihilation process should be greatly enhanced at large x_T , compared to π^+P collisions and should contribute substantially to the direct photon cross-section. However in the x_T range covered by the experiments the Compton term (identical for π^-P and π^+P reactions) contributes predominantly to the cross-section. Differences are expected to be small and difficult to exhibit. NA24 has observed a larger direct photon cross section in π^-P collisions than in π^+P collisions (Fig.8.a). WA70 has observed a slightly higher γ/π^0 ratio in π^-P interactions compared to π^+P (Fig.8.b). These ratios obtained by the two experiments are compatible with the theoretical expectation but deviation from unity has a small statistical significance.

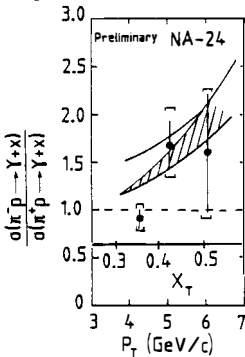


Fig. 8.a: π^-/π^+ beam ratio for NA24. The upper curve is taken from ref. 21 while the dashed band is taken from ref. 22.

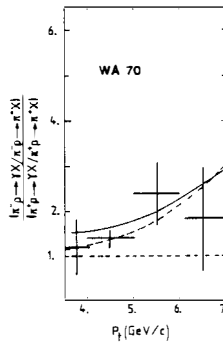


Fig. 8.b: π^-/π^+ beam ratio for WA70. The upper curve is taken from ref. 21 while the dashed curve is taken from ref. 22.

At the ISR, no significant difference is observed between PP and $P\bar{P}$ collisions (Fig. 6). It should be mentioned that at the highest P_T measured the annihilation term should contribute at most for 25% to the direct γ cross-section (R808 has not observed any difference in the production of π^0 between PP and $P\bar{P}$ collisions).

In conclusion to this section, better statistics are needed for a clear observation of the annihilation contribution.

IV.3. CORRELATIONS

The measurement of the distribution of particles densities, as a function of the azimuthal angle ϕ relative to the photon direction, should provide informations on the direct photon production mechanism. Except for bremsstrahlung contributions, prompt photons should not be accompanied by particles along their direction. The Compton process produces a direct photon in association with a quark jet in the opposite direction, whereas in the annihilation process a direct photon is associated with a gluon jet.

Both NA24 and WA70 have measured the particle density as a function of azimuth. Distribution are shown in Fig. 9 for direct γ 's and π^0 's. The difference on the trigger side ($\Delta\phi \approx 0^\circ$) suggests that bremsstrahlung contribution to direct photon production is small, and γ 's are well isolated whereas π^0 's are part of jet fragments. On the away side ($\Delta\phi \approx 180^\circ$) no significant difference is observe between γ 's and π^0 's. Similar results have been obtained by the R807 experiment at the ISR²³⁾.

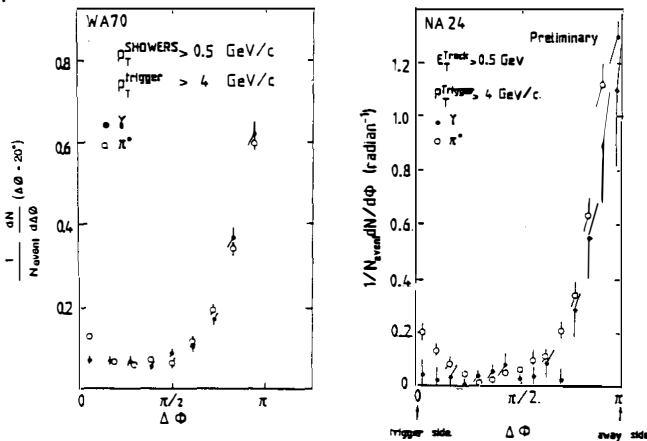


Fig. 9: Particle density associated with a high P_T direct photon as measured by NA24 and WA70.

IV.4. CROSS-SECTIONS

As mentioned in the introduction, direct photon cross-sections have been calculated to next-to-leading order^{2,3}). They are about a factor of 2 higher than leading order cross-sections.

Prompt γ physics has become an excellent quantitative testing ground of QCD, though experimental measurements are difficult and the yield is small. Cross section measured by the NA3 and the R806 experiments are in agreement with next-to-leading order calculations²⁴). Recently NA24 and UA2 have measured the direct-photon production cross-section.

NA24 results are shown on Figure 10, for π^-P , π^+P and PP interactions, together with a next-to-leading order calculation of Aurenche et al. ; a remarkable agreement between data and theory is obtained.

UA2 has measured the direct photon production cross-section in two different pseudorapidity intervals ($|\eta| \leq 0.85$, $1.1 \leq |\eta| \leq 1.7$). Figure 11 compares the results and a next-to-leading order prediction of Aurenche et al.²⁵) (upper curve). The lower curve corresponds to the same prediction but excluding bremsstrahlung contributions with an angle less than 45° , in order to simulate the effect of the isolation criteria which reject a photon too close to a jet or within a jet. Again a remarkable agreement is obtained. One can notice the high values of P_T obtained (up to 50 GeV/c); it corresponds however to low x_T (0.15 at maximum) a region where the Compton contribution dominates over the annihilation (up to $P_T \approx 60$ GeV/c). On the same figure, the measured π^0 cross-section in the Forward/Backward regions is also shown.

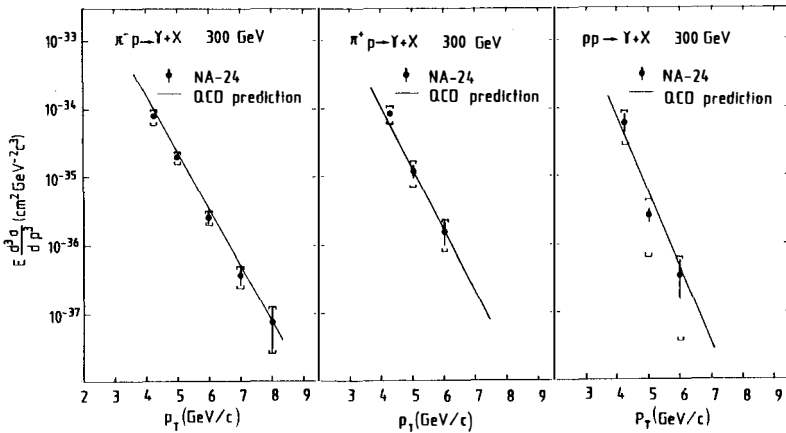


Fig. 10: Direct photon cross-sections for three incident beams as measured by NA24. The solid lines represent a QCD calculation from ref. 21. A 2% systematic uncertainty on the energy scale has not been included in the error bars. The systematic errors (brackets) which are due to the uncertainty on the Monte-Carlo background estimation are added linearly to the statistical errors.

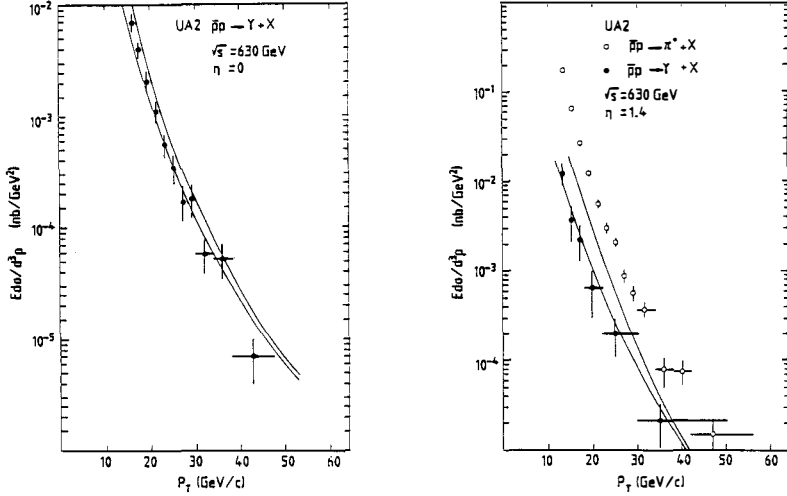


Fig. 11: The invariant inclusive cross-section for direct photon production (black dots) as at $\eta=0$ and at $1.1 \leq |\eta| \leq 1.7$ as measured in UA2. Upper curves show prediction from ref. 25, lower curves result from excluding bremsstrahlung photon with quark-photon angle less than 45° . A 20% systematic uncertainty as not been include in the error bars. Also shown the invariant π^0 cross-section for production at $1.1 \leq |\eta| \leq 1.7$.

Since many measurements are now available at different center of mass energies and different rapidities, one would like to compare them to calculations using different parametrizations of the gluon structure function in order to choose among them.

IV.5. γ /JET RATIO

UA2 has measured the ratio of the direct photon cross section to the jet cross section, in the P_T range between 30 and 50 GeV/c :

$$\sigma_\gamma/\sigma_{\text{jet}} = 2.9 \pm 0.9 \text{ (stat.)} \pm 1.2 \text{ (syst.)} 10^{-4}$$

where the systematic errors are due to the uncertainty of the jet energy scale²⁶). In this P_T range a lowest order QCD calculation using different parametrizations of the structure function predicts a ratio in the range between 3 and $4.5 \cdot 10^{-4}$. It is interesting to note that the γ /jet ratio found at the ISR²⁷), for different values of $P_T(x_T)$, has a similar value, approximately 10^{-4} .

V. CONCLUSIONS

A clear direct photon signal has been observed by all experiments (NA24,R808,UA2 and WA70) over a large range of center of mass energies (from $\sqrt{s} = 23$ GeV to 630 GeV), for different rapidities and in many different reactions (π^+P , π^+P , PP and $P\bar{P}$).

Results are in agreement with theory concerning : cross-sections, beam ratios and γ /jet ratio.

More statistics are needed to give information on the gluon structure and fragmentation functions, the bremsstrahlung contribution and to separate the annihilation from the Compton contribution.

ACKNOWLEDGMENTS

I would like to acknowledge K. Pretzl, P. Seyboth, J. Thompson and M. Werlen for their cooperation and useful discussions in preparing this review.

REFERENCES AND FOOTNOTES

- 1) F. Halzen and D. M. Scott, Phys. Lett. 140B (1984) 87.
R. Horgan and M. Jacob, Nucl. Phys. B179 (1981) 441.
E. L. Berger, E. Braaten and R.D. Field, Nucl. Phys. B239 (1984) 52.
T. Ferbel and W.R. Molzon, Rev. Mod. Phys., 56 (1984) 181.
- 2) P. Aurenche and J. Lindfors, Nucl. Phys. B168 (1980) 296;
P. Aurenche et al., Phys. Lett. 140B (1984) 87.
- 3) A.P. Contogouris et al., Phys. Rev. D25 (1982) 1280, Phys. Rev. D26 (1982) 1618; Phys. Rev. D29 (1984) 2527.
- 4) NA24 Collaboration, A. Bamberger et al., CERN/SPSC/80-83, CERN/SPSC/83-3
- 5) WA70 Collaboration, L. Bachman et al., CERN/SPSC/80-61
- 6) R808 Collaboration, E. Anassantizis et al., CERN/ISRC/81-16
- 7) The AFS detector:
H. Gordon et al., Nucl. Inst. Meth. 196 (1982) 303;
O. Botner et al., Nucl. Inst. Meth. 196 (1982) 314;
O. Botner et al., Nucl. Inst. Meth. 179 (1981) 45.
- 8) UA2 Collaboration, M. Banner et al., CERN/SPSC/78-54
- 9) C. De Marco et al., Nucl. Inst. Meth. 217 (1983) 405;
V. Artemiev et al., Nucl. Inst. Meth. 224 (1984) 408.
- 10) L. Bachman et al., Nucl. Instr. Meth. 206, 85 (1983).
- 11) R. Batley et al., Nucl. Instr. Meth. 242, 75 (1985).
- 12) B. Mansoulié, in Proc. of the 3rd Moriond workshop on $P\bar{P}$ physics, page 609, Editions Frontières 1983;
M. Dialinas et al., LAL-RT/83-14 (ORSA Y, 1983);
K. Borer et al., Nucl. Inst. Meth. 227 (1984) 29.
- 13) NA24 Experiment:
K. Pretzl, XVI Symposium on Multiparticle Dynamics, Kiryat-Anavim, Israel, 1985.
K. Pretzl, Proc. of the XII International Conference on High Energy Physics, Leipzig, Vol. I (1984) 283;
P. Seyboth XV International Symposium on Multiparticle dynamics, Lund (1984) page 596;
A. Bamberger, Proc. of the XX Rencontre de Moriond (1985).
R808 Experiment:
T. Åkesson et al., Phys. Lett. 158B (1985) 282;
H. Breuer, Proc. of the XX Rencontre de Moriond 1985.
WA70 Experiment:
M. Bonesini et al., Prompt photons production by π^- and π^+ on protons at 280 GeV/c, contributed papers P13-4; HEP85 Bari and 308, ISLEPH85 Kyoto.
- 14) R. Ford and W. Nelson, SLAC-210 (1978).
- 15) For a pure sample of single photons ϵ_{γ} depends on the converter thickness and on the preshower counter threshold (T). In the central preshower detector T is set at 2 mips with a converter thickness of 1.5 X_0 , ϵ_{γ} is then roughly independent of energy in the range considered. In the Forward/Backward regions, T is set at 6 mips, with a converter thickness of 1.4 X_0 , resulting in a dependence of ϵ_{γ} upon energy which has to be taken into account.
- 16) UA2 Collaboration, M. Banner et al., Z. Phys. C27 (1985) 329.

- 17) F. Paige and S. Protopopescu, BNL/81-31987.
- 18) O. Benary, E. Gostman and D. Lissauer, Z. Phys. C16 (1983) 211.
- 19) D.W. Duke and J.F. Owens, Phys. Rev. D30 (1984) 49.
- 20) R. Baier et al., Z. Phys. C2 (1979) 265.
- 21) Ref. 2 and private communication.
- 22) Ref. 3, A. P. Contogouris et al., McGill preprint to be published, Phys. Rev. D32 (1985) 1134.
- 23) M. Diakonou et al., Phys. Lett. 91B (1980) 301;
T. Åkesson et al., Phys. Lett. 118B (1982) 178;
C. Kourkouvelis et al., Nucl. Phys. B179 (1981) 1;
A.L.S. Angelis et al., Phys. Lett. 98B (1981) 115.
- 24) NA3 Collaboration: J. Badier et al., CERN-EP/85-200.
R806 Collaboration: E. Anassonizis et al., Z. Phys. C13 (1982) 277.
- 25) P. Aurenche private communication.
- 26) J.A. Appel et al., Phys. Lett. 160B (1985) 349.
- 27) V. Burkets, Proc. of the XVIII Rencontre de Moriond (1983);
R. Moller, Acta. Phys. Pol. B15 (1984) 989.

TABLE 1

EXPERIMENT	NA24	WA70	R808	UA2
REACTION	300 GeV/c beams π^- , π^+ , P on H_2 target	280 GeV/c beams π^- , π^+ , P on H_2 target	$\sqrt{s} = 53$ GeV PP, PP	$\sqrt{s} = 630$ GeV PP
KINEMATICAL RANGE	$-0.6 < y^* < 0.55$	$ x_F < 0.45$	$ y \leq 0.4$	$ y \leq 0.85$ $1.1 \leq y \leq 1.7$
P_T RANGE	4 - 7 GeV/c	4 - 7 GeV/c	3 - 6 GeV/c	12 - 50 GeV/c
σ/\sqrt{E}	0.28	$0.15 + 0.04\sqrt{E}$	0.09-0.06	0.15
METHOD	DIRECT	DIRECT	DIRECT	CONVERSION
$\sigma(M_{\pi^0})$	15 MeV	12 MeV	15 MeV	/